Check for updates

# Two Calix[3]Phenothiazine-Based Amorphous Pure Organic Room-Temperature Phosphorescent Supramolecules Mediated by Guest

*Yonghui Sun, Linnan Jiang, Lijuan Liu, Yong Chen, Wen-Wen Xu, Jie Niu, Yuexiu Qin, Xiufang Xu, and Yu Liu\**

**Herein, two kinds of amorphous solid-state supramolecular systems with purely organic room temperature phosphorescence (RTP) from calix[3] phenothiazine (C[3]Pz) activated by 1,2-/1,3-dicyanobenzene (1,2-/1,3-DCB) are reported. Different from macrocycle-confined guest phosphorescence emission, RTP of these two amorphous solid-state supramolecular systems is entirely from the 1,2-/1,3-DCB rivets C[3]Pz cavity to form dense supramolecular complex through C—H···π interactions, leading to two different phosphorescence emissions at 566/524 nm under 430 nm excitation, respectively. Although C[3]Pz shows a regular arrangement in the crystal, the vibration dissipation of the benzene ring results in C[3]Pz emitting only fluorescence at 508 nm at room temperature. 1,2-DCB and 1,3-DCB can act as molecular rivets to fix the C[3]Pz to inhibit molecular vibration so as to reduce nonradiative relaxation, which enables C[3]Pz to achieve effective RTP emission with 20.8–36.8% quantum yields. This kind of guest-activated host RTP, which is fairly rare in supramolecular systems, is successfully used for color QR codes and information encryption.**

## 1. Introduction

Recently, purely organic room temperature phosphorescence (RTP) has attracted extensive attention due to its great potential application in the fields of organic optoelectronic materials and bioimaging.[1–4] Unlike fluorescence, organic phosphorescence is rarely achieved at room temperature. Because of the inefficient spin-orbit coupling (SOC) of pure organic molecules, triplet excitons are easily deactivated through thermal vibrational and collisional processes or invasion of moisture and oxygen.[5–9] Generally, to achieve high-efficiency RTP, two conditions need to be met, one is to improve the inter-system crossing efficiency, and the other is to suppress the non-radiative relaxation process.[10–14] Based on this, many interesting RTP systems have been developed through rational design in the past few years.[15–18] For example, the introduction of heavy atoms or carbonyl and groups containing other heteroatoms with abundant lone-pair electrons into organic molecules can effectively increase the SOC constant, thereby achieving efficient intersystem crossing (ISC).[19–23] In addition, by introducing intermolecular charge-transfer states in single-component crystals and multi-component doping systems, the singlet-triplet energy gap can be minimized to accelerate the ISC rate to achieve phosphorescence emission.[24–27] At the same time, many brilliant strategies such as molecular aggregation (including H-aggregation, $\pi$–$\pi$ stacking, and n–$\pi$ stacking),[28–31] crystallization,[32–35] polymerization,[36–39] host–guest complexation,[40,41] carbon dots and clusterization-triggered emission have also been used to construct RTP systems.[42,43] Despite the exciting development of RTP, so far, most RTP systems for pure organic compounds have been realized in the crystal state, and the demanding growth condition and uncontrollable growth process required for crystal cultivation have hindered their practical application to a certain extent. Therefore, it is imperative to design and develop a facile and general strategy to obtain amorphous pure organic compounds with efficient RTP emission.

In supramolecular chemistry, the assembly strategy of host–guest complexation has excellent advantages in the fabricating of tunable and smart organic luminescent materials in aqueous media and the solid state.[44–47] In recent years, there have been more and more studies using the cavity confinement effect of the macrocycle (especially for cyclodextrin and cucurbituril) to induce organic single-molecule phosphorescence emission.[48–50] For example, our group reports an unprecedented enhancement of the phosphorescence quantum yield of bromophenyl-methyl-pyridinium chloride from 2.6% to 81.2% by complexing with cucurbit[6]uril.[51] However, there are few reports showing that organic single molecules induce phosphorescence of macrocycles in host–guest complexes because the charge

Y. Sun, L. Jiang, L. Liu, Y. Chen, W.-W. Xu, J. Niu, Y. Qin, X. Xu, Y. Liu
College of Chemistry
State Key Laboratory of Elemento-Organic Chemistry
Nankai University
Tianjin 300071, P. R. China
E-mail: yuliu@nankai.edu.cn
Y. Liu
Collaborative Innovation Center of Chemical Science and Engineering
Tianjin 300071, P. R. China

transfer between the host and guest usually quenches the phosphorescence upon complex formation.[52] In this regard, the introduction of small organic molecules may break this stereotype of host-induced guest phosphorescence emission and realize guest-activated host phosphorescence emission.

Herein, we developed a new strategy to develop amorphous purely organic compounds with efficient RTP emission by introducing different non-phosphorescent guest molecules into calix[3]phenothiazine (**C[3]Pz**), which can effectively suppress the nonradiative relaxation process and enhance the quantum yield, named as guest activated RTP (**Scheme 1**). Due to the lack of ISC channel to the triplet state, **C[3]Pz** emits fluorescence only at 508 nm at room temperature. When the temperature decreases to 77 K, **C[3]Pz** shows double phosphorescence emission at 524 and 566 nm, respectively. To improve the phosphorescence behavior, we introduce electron-withdrawing-based non-phosphorescence guest molecules, aiming to investigate how the guest molecules influenced the phosphorescence behavior of **C[3]Pz**. It was found that **C[3]Pz** could serve as a macrocyclic donor to encapsulate 1,2-dicyanobenzene (**1,2-DCB**) and 1,3-dicyanobenzene (**1,3-DCB**) in the solid state. Notably, the encapsulated **1,2-DCB** and **1,3-DCB** confined the vibrations of the **C[3]Pz**, suppressed the non-radiative transition, and enhanced the ISC rate, which induces the RTP of **C[3]Pz** at 566 nm and 524 nm, respectively. It is noteworthy that macrocyclic compounds with effective RTP emission activated by guest molecules have not been reported so far (**Scheme 1**).

## 2. Results and Discussion

### 2.1. Characteristics and Photophysical Properties of C[3]Pz

Phenothiazine is a well-known building block to achieve the good communication between singlet and triplet states, because the existence of O or N atoms with lone pair electrons is capable of promoting n–$\pi^*$ transitions to populate triplet excitons.[53,54] In this research, pure 10-phenylphenothiazine has only a blue fluorescence band at 445 nm under UV excitation, no phosphorescence was observed at room temperature.[54] But here we were curious about the cyclization luminescent behavior of 10-phenylphenothiazine, because it has been reported that through cyclization, the energy gap between the singlet and triplet states can be reduced, resulting in excellent ISC efficiency.[56] **C[3]Pz** was accessed in a facile two-step synthesis and unambiguously characterized by $^1$H NMR, $^{13}$C NMR, and HRMS spectra (Figures S1–S5, Supporting Information). **Figure 1**a,b shows the absorption and emission spectra of **C[3]Pz** in the solid state and in dichloromethane solution at 298 K. At room temperature, **C[3]Pz** exhibited a fluorescence emission at 508 nm in the solid state with a lifetime of 10.9 ns (Figure 1c). In dichloromethane, **C[3]Pz** exhibits dual fluorescence emission at 427 and 450 nm. Notably, in the solid state, **C[3]Pz** exhibits excitation-dependent emission at excitation wavelengths ranging from 380 to 430 nm, indicating the conformational flexibility of **C[3]Pz** (Figure 1d).
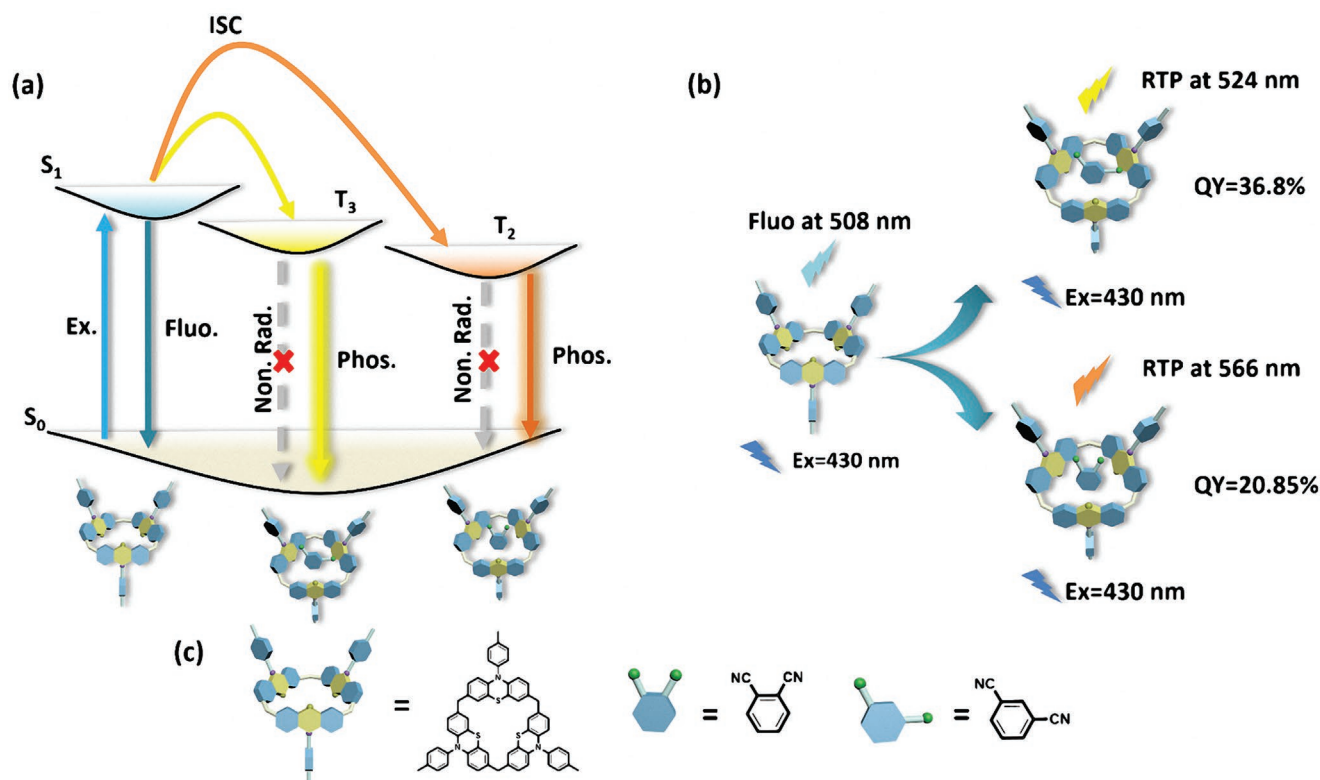


**Scheme 1.** a) Schematic illustration of the RTP emission. b) Schematic illustration of the RTP emission of selectively activated **C[3]Pz**. c) Molecular structures of fluorescent guest molecule (1,2-dicyanobenzene, 1,3-dicyanobenzene) and RTP emissive **C[3]Pz**.
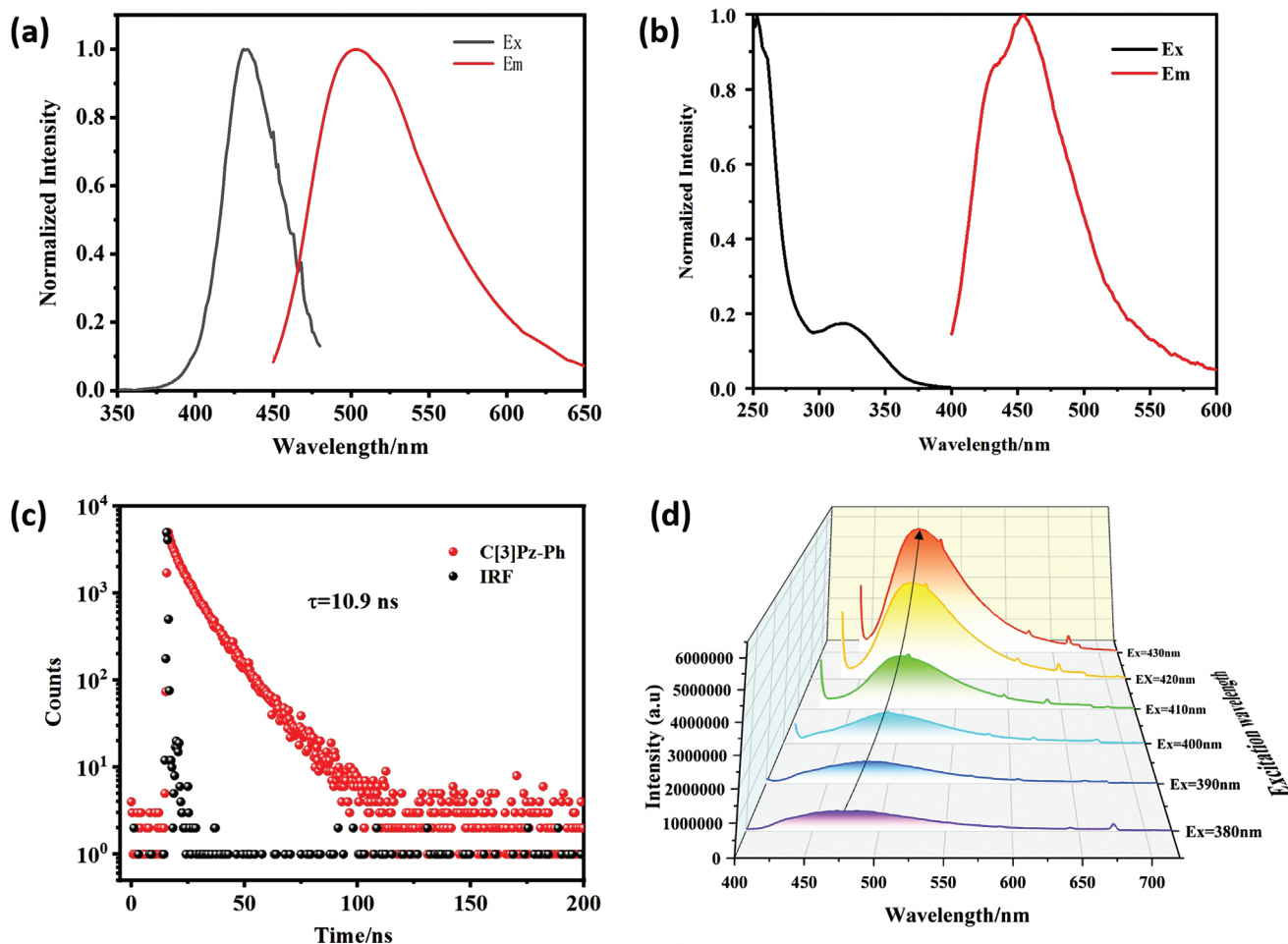
**Figure 1.** a) Absorption and photoluminescence spectra of **C[3]Pz** in the solid state at 298 K. b) Absorption and photoluminescence spectra of **C[3]Pz** in dichloromethane solution at 298 K ([C[3]Pz] = $1 \times 10^{-4}$ м), the excitation of **C[3]Pz** was 320 nm. c) Luminescent delay lifetimes of **C[3]Pz** at 508 nm. IRF, instrument response function. d) Excitation-dependent emission of **C[3]Pz** under ambient conditions.

When the temperature was cooled to 77 K, **C[3]Pz** exhibited fluorescence (508 nm) and dual phosphorescence (524 nm, 566 nm) according to its steady-state photoluminescence (**Figure 2**a). Figure 2b described the time-resolved (at fixed delay of 100 μs) emission spectra, where the steady-state emission band at 508 nm disappeared completely for its short lifetime. The transient decay profile at 524 and 566 nm was also investigated by varying the temperature from 127 to 298 K to verify the emission nature. Photoluminescence intensity and lifetime showed a decreasing trend with increasing temperature, suggesting that phosphorescence is the dominant radiation decay channel at 524 and 566 nm (Figure 2c,d). As the temperature decreases from 297 to 127 K, the lifetime of **C[3]Pz** increases to 95 ms at 524 nm and 92 ms at 566 nm (**Table 1**). Apparently, **C[3]Pz** exhibits obvious phosphorescence emission only at low temperature, and the phosphorescence efficiency of **C[3]Pz** at room temperature is unsatisfactory. To obtain higher phosphorescence efficiency at room temperature without changing the structure, we then explored the possibility of guest-induced phosphorescence property of **C[3]Pz**.

## 2.2. Photophysical Properties of C[3]Pz@1,2-DCB

As a guest molecule with strong electron-withdrawing ability, 1,2-dicyanobenzene (**1,2-DCB**) is expected to form host–guest complex with macrocyclic donor **C[3]Pz**, thus affecting its optical properties without changing the structure of **C[3]Pz**. Dissolving equimolar **C[3]Pz** and **1,2-DCB** in $CH_2Cl_2$, and then volatilizing the solvent naturally at room temperature can give the host–guest complex. As shown in the **Figure 3**a, the obtained **C[3]Pz@1,2-DCB** powder is obviously different from **C[3]Pz**, and shows bright orange under UV light, which is in sharp contrast with the cyan of **C[3]Pz**. In order to understand this phenomenon, their photophysical properties at room temperature were explored. As shown in the Figure 3b, compared with **C[3]Pz**, the UV–vis absorption spectra of **C[3]Pz@1,2-DCB** has a red-shifted of nearly 10 nm. Correspondingly, the emission band of **C[3]Pz@1,2-DCB** at 566 nm has a significant red-shifted of 58 nm compared with that of **C[3]Pz** at 508 nm. Interestingly, the emission band of **C[3]Pz@1,2-DCB** at 566 nm is highly consistent with the phosphorescent emission of **C[3]Pz** at 566 nm at 77K, implying that the guest molecule
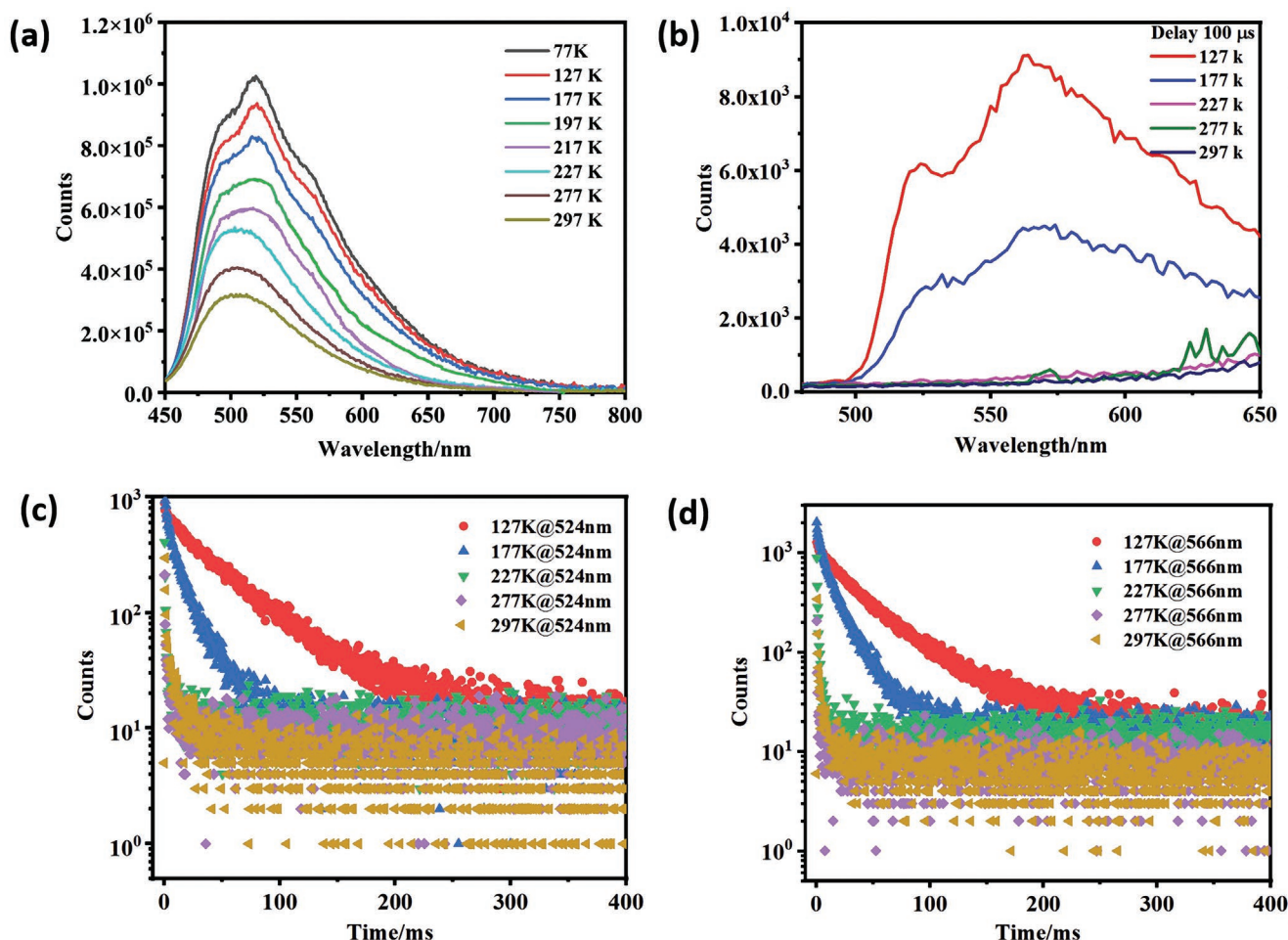
**ADVANCED
SCIENCE NEWS**

www.advancedsciencenews.com

**ADVANCED
OPTICAL
MATERIALS**

www.advopticalmat.de

**Figure 2.** a,b) Steady-state photoluminescence spectra from 77 to 297 K and delayed (delay = 100 µs) photoluminescence spectra from 127 to 297 K. c,d) Temperature-dependent transient photoluminescence decay of **C[3]Pz**.

**1,2-DCB** induces phosphorescent emission of **C[3]Pz** at 566 nm at room temperature. The time-resolved photoluminescence spectra of **C[3]Pz@1,2-DCB** shows that the spectral position and profile under 100 µs delay are highly overlapped with the steady-state photoluminescence spectra (Figure 3c). In addition, the transient photoluminescence decay spectrum of **C[3]Pz@1,2-DCB** at room temperature shows a lifetime of 0.98 ms, which implies the attribution of phosphorescence (Figure S6).

**Table 1.** Photophysical data of **C[3]Pz**, **C[3]Pz@1,2-DCB**, and **C[3]Pz@1,3-DCB**.

| Compound | $T$ [K] | $\lambda_{em}$ [nm] | PL | $\tau_p$ | $\Phi_p$ [%] |
|---|---|---|---|---|---|
| **C[3]Pz** | 298 | 508 | Fluo | 10.9 ns | – |
| | 77 | 508 | Fluo | – | – |
| | | 524 | Phos | 95 ms | – |
| | | 566 | Phos | 92 ms | - |
| **C[3]Pz@1,2-DCB** | 298 | 566 | Phos | 0.98 ms | 36.8 |
| | 77 | 566 | Phos | 46 ms | – |
| **C[3]Pz@1,3-DCB** | 298 | 524 | Phos | 0.52 ms | 20.8 |
| | 77 | 524 | Phos | 51 ms | – |

In order to further determine the luminescence properties of **C[3]Pz@1,2-DCB**, we carried out temperature dependent photoluminescence spectroscopy experiments. As shown in the Figures S7–S8 (Supporting Information), the experiment shows that in the temperature range of 77–297 K, the emission bands of **C[3]Pz@1,2-DCB** steady-state photoluminescence spectra and time-resolved photoluminescence spectra are both stable at 566 nm, and with the temperature decreasing, the intensity gradually increases, and the photoluminescence life decay curve also shows the same property, that is, the phosphorescence life gradually increases with the temperature decreasing (Figure S9, Supporting Information). The phosphorescence quantum yield of **C[3]Pz@1,2-DCB** under atmosphere is further determined as 20.8% (Figure S10, Supporting Information). These results indicate that the guest molecule **1,2-DCB** induces the phosphorescent emission of **C[3]Pz** at 566 nm at room temperature.

## 2.3. Photophysical Properties of C[3]Pz@1,3-DCB

To verify the RTP of **C[3]Pz** activated by guest molecules, we selected **1,3-DCB** as the guest molecule, and further investigated its influence on the phosphorescence behavior of **C[3]Pz**.
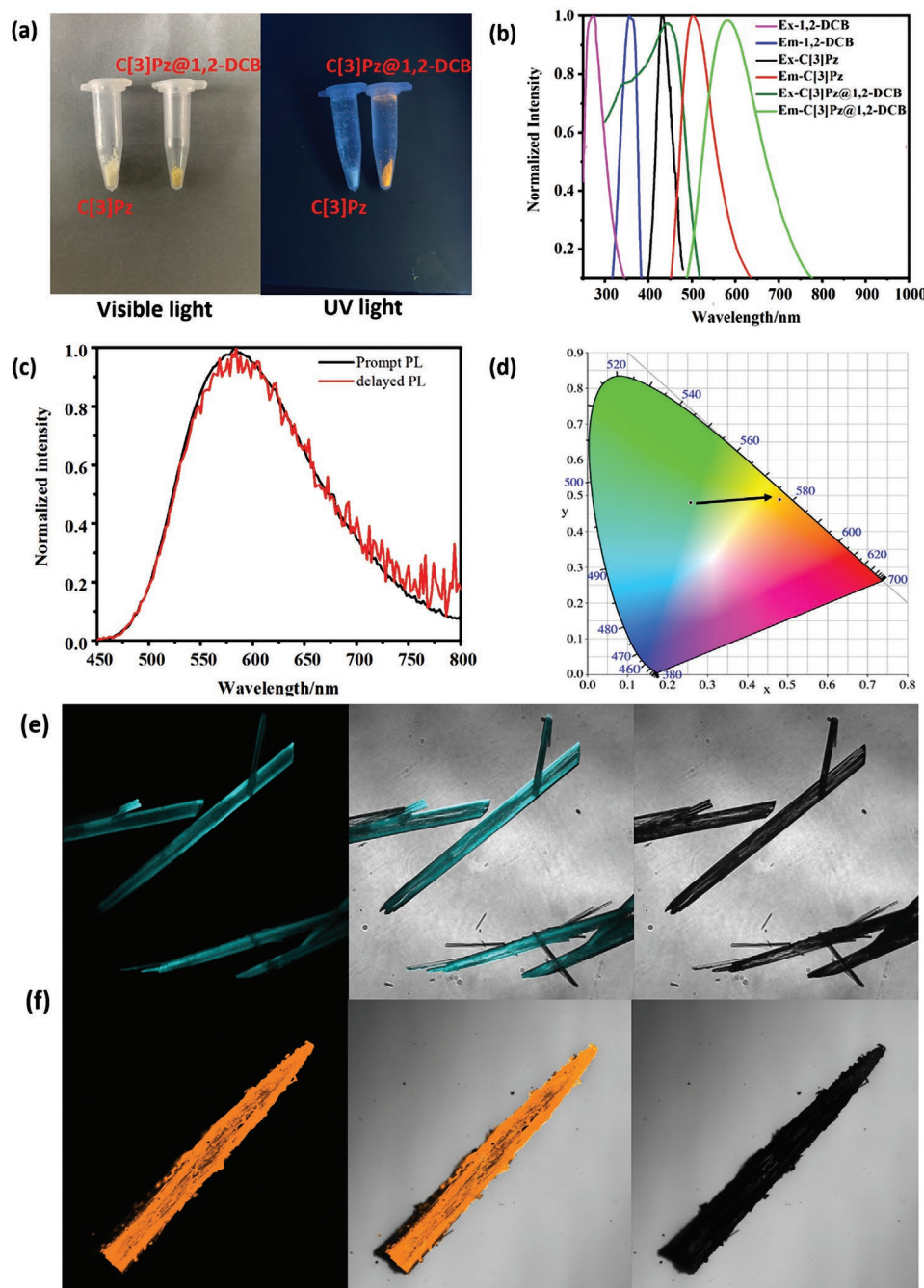
**Figure 3.** a) Photographs of the solid powder of **C[3]Pz** and **C[3]Pz@1,2-DCB** under visible light and 365 nm UV light. b) Absorption and photoluminescence spectra of **1,2-DCB**, **C[3]Pz**, and **C[3]Pz@1,2-DCB**. The excitation and emission wavelength of **1,2-DCB** was 288 and 360 nm in solid state at 298 K, respectively. The excitation and emission wavelength of **C[3]Pz** was 430 and 508 nm in solid state at 298 K, respectively. The excitation and emission wavelength of **C[3]Pz@1,2-DCB** was 430 and 566 nm in solid state at 298 K, respectively. c) Prompt and delayed phosphorescence spectra of **C[3]Pz@1,2-DCB**. Excitation by 430 nm, delayed time: 100 µs. d) The CIE coordinate of **C[3]Pz** and **C[3]Pz@1,2-DCB** according to the CIE 1931 chromaticity. e,f) LSCM images of **C[3]Pz** and **C[3]Pz@1,2-DCB**.

Unlike **1,2-DCB**, **1,3-DCB** shows bright yellow light after volatilizing the equimolar solution of **C[3]Pz** and **1,3-DCB** (Figures S11 and S12, Supporting Information). Similarly, we studied the photophysical properties of **C[3]Pz@1,3-DCB** at room temperature. The UV absorption maximum of **C[3]Pz@1,3-DCB** has a red shift of 7 nm compared with the **C[3]Pz**, and the

photoluminescence steady state spectrum shows an emission of 524 nm, i.e., a red shift of 16 nm compared with that of **C[3]Pz** (Figures S13 and S14, Supporting Information). To our surprise, the emission band of **C[3]Pz@1,3-DCB** at 524 nm is highly consistent with the phosphorescence emission band of **C[3]Pz** at 77K. In addition, the contour and position of the

**ADVANCED
SCIENCE NEWS**

www.advancedsciencenews.com

**ADVANCED
OPTICAL
MATERIALS**

www.advopticalmat.de

time-resolved photoluminescence spectrum of **C[3]Pz@1,3-DCB** highly overlap with the steady-state spectrum, accompanied by a lifetime of 0.52 ms (Figures S15 and S16, Supporting Information). These results mean that **1,3-DCB** induces room temperature phosphorescence of **C[3]Pz**. In order to further determine the luminous characteristics of **C[3]Pz@1,3-DCB**, variable temperature spectrum experiments were carried out. The experiments showed that in the temperature range of 77 K-297 K, the emission intensity of **C[3]Pz@1,3-DCB** steady-state photoluminescence spectrum and time resolved photoluminescence spectrum at 524 nm gradually increased with the decrease of temperature, and the photoluminescence life decay curve also gradually increased with the decrease of temperature, thus eliminating the possibility of thermal activation of delayed fluorescence (Figures S17–S19, Supporting Information). In addition, the phosphorescence quantum yield of **C[3]Pz@1,3-DCB** is determined as 36.8% (Figure S20, Supporting Information).

### 2.4. Host-guest Chemistry and Theoretical Research

The excellent photophysical properties of **C[3]Pz@1,2-DCB** and **C[3]Pz@1,3-DCB** encourage us to further study the host-guest

chemistry between guest molecules and **C[3]Pz**. The host–guest interaction in the liquid phase was studied by NMR titration in $CD_2Cl_2$ or $CDCl_3$. The experiment showed that both **1,2-DCB** and **1,3-DCB** had too weak interaction with **C[3]Pz** in $CD_2Cl_2$ or $CDCl_3$, so that no obvious chemical shift was observed (Figures S21–S24, Supporting Information). Subsequently, we studied the host–guest interaction in the amorphous state by PXRD and solid-state NMR. PXRD experiment analyzed the structural changes of **C[3]Pz** after interaction with two guest molecules, in which varying degrees of changes before and after interaction with guest molecules were observed, proving that a solid supramolecular complex appeared (**Figure 4**a and Figure S25, Supporting Information). The solid-state NMR experiment showed that the strong interaction between host and guest almost completely shields the signal of guest molecules, and the signal of **C[3]Pz** after interaction with guest molecules has been enhanced to varying degrees and has obvious upfield shifts (Figure 4b,c and Figure S26, Supporting Information). Therefore, there is a strong interaction between **C[3]Pz** and guest molecules in solid state.

The X-ray single crystal diffraction experiment confirmed that the **C[3]Pz** solid state shows a partial-cone conformation. By slowly evaporating the **C[3]Pz** solution of ethyl acetate/petroleum
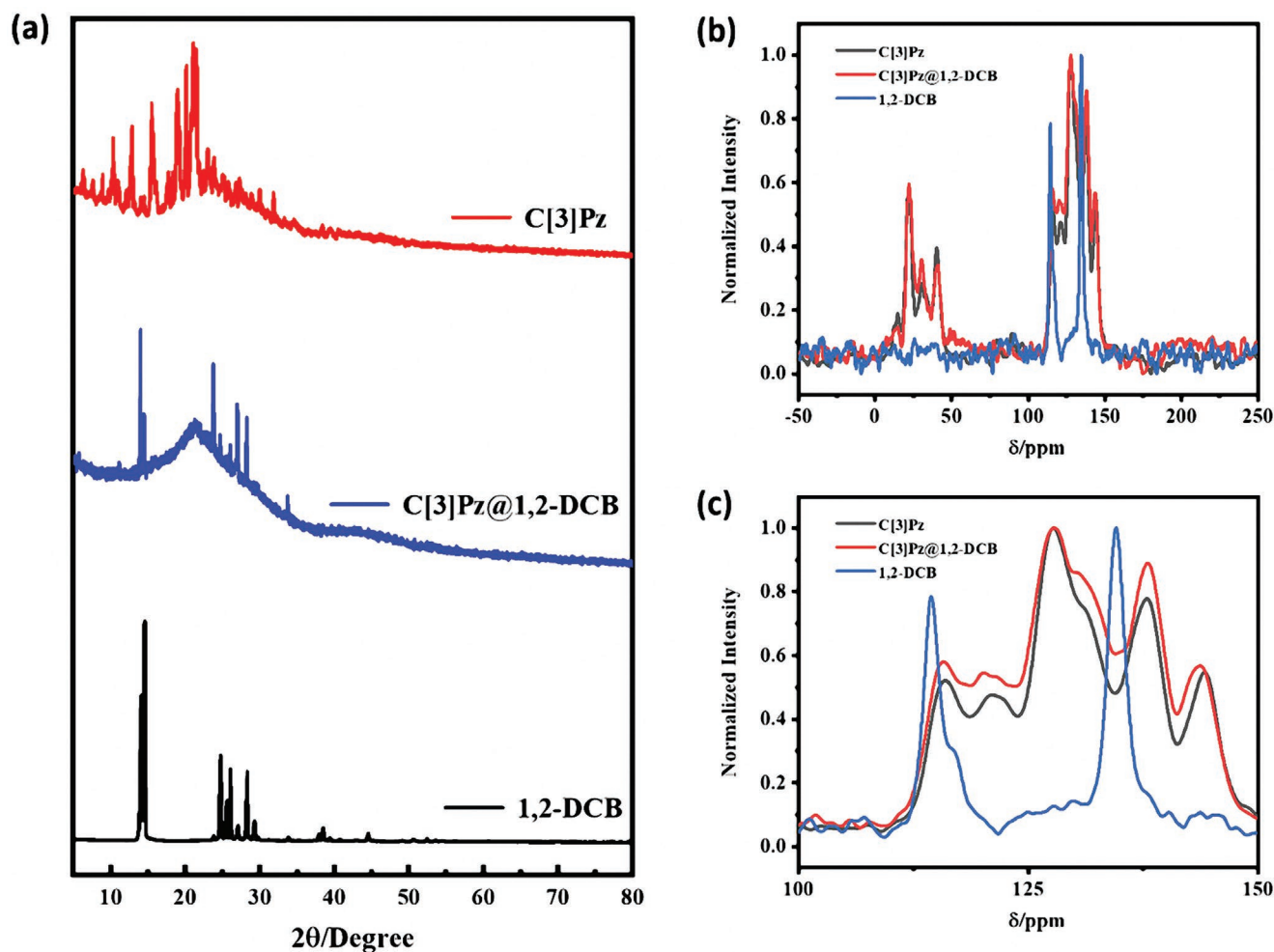


**Figure 4.** a) PXRD patterns of **1,2-DCB**, **C[3]Pz**, and **C[3]Pz@1,2-DCB**. b) 400 MHz Solid-state NMR spectra of **1,2-DCB**, **C[3]Pz** and **C[3]Pz@1,2-DCB**. c) Partial solid-state NMR spectra of **1,2-DCB**, **C[3]Pz** and **C[3]Pz@1,2-DCB** from 100 to 150 ppm.

ADVANCED
SCIENCE NEWS
www.advancedsciencenews.com

ADVANCED
OPTICAL
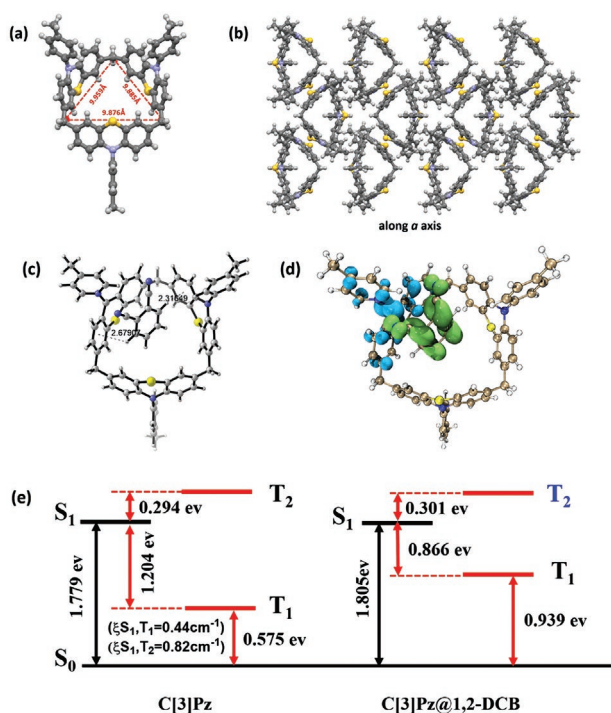MATERIALS
www.advopticalmat.de

**Figure 5.** a) Crystal structures of **C[3]Pz** solvents are omitted for clarity. b) Space-fill structures shown along a axis. solvents are omitted for clarity. c) Optimized molecular geometries of **C[3]Pz@1,2-DCB**. d) Real space representation of hole and electron distributions of **C[3]Pz@1,2-DCB**. Green and blue regions denote the electron and hole distributions, respectively. e) Energy-level diagrams in **C[3]Pz** and **C[3]Pz@1,2-DCB**.

ether, a single crystal with partial-cone conformation of **C[3]Pz** was obtained. The butterfly shaped **C[3]Pz** has a cavity close to 1 nm. The crystal packing mode shows that **C[3]Pz** forms an infinite one-dimensional channel structure along the *a* axis, which makes it possible to wrap guest molecules (**Figure 5**a,b). Thanks to the electron donating ability of N and S atoms, we speculate that **1,2-DCB** or **1,3-DCB** enter the cavity of **C[3]Pz** to form host–guest complexes. This conjecture was confirmed by density functional theory (DFT) calculation with Gauss 16 program. The results show that the stoichiometric 1:1 host–guest complex has the minimum binding energy (−32.7 kcal mol$^{-1}$, Table S1, Supporting Information), which is considered to be the most stable molecular geometry. From the optimized molecular structure, it can be seen that there are extensive C−H···$\pi$ interactions (with the distance of 2.316 Å, 2.679 Å) in **C[3]Pz@1,2-DCB** (Figure 5c). In addition, hole–electron analyses were carried out for the obtained inclusion complexes. As shown in Figure 5d, electrons were transferred from electron-rich **C[3]Pz** to electron deficient **1,2-DCB** in the excited state. This intermolecular charge transfer led to the reduction of $\Delta E_{ST}$ of **C[3]Pz@1,2-DCB**, changing from the initial 1.204 to 0.866 eV compared with **C[3]Pz** (Figure 5e). Although this is conducive to phosphorescent emission, the calculation shows that the most likely intersystem crossing of **C[3]Pz@1,2-DCB** is (T$_2$→S$_0$), corresponding to the phosphorescent emission wavelength of 586 nm, which is only 20 nm different from the experimental data. On the other hand, **1,2-DCB**, as a molecular rivet, can well inhibit the vibration rotation of the benzene ring on **C[3]Pz**,

which to a large extent stabilizes the triplet excitons and inhibits the non-radiative transition of **C[3]Pz**, thus achieving phosphorescent emission. In addition, the most stable molecular geometry of **C[3]Pz@1,3-DCB** has been optimized. As shown in the Figure S25 (Supporting Information), the widespread C−H···$\pi$ interaction (with the distance of 2.524, 2.600, and 4.296 Å) makes the host–guest complex very stable and has the minimum binding energy (−29.5 kcal mol$^{-1}$, Table S1, Supporting Information). The results of hole–electrons analyses are similar to those of **C[3]Pz@1,2-DCB**, showing the charge transfer from **C[3]Pz** to **1,3-DCB** (Figure S27, Supporting Information). The intersystem crossing of **C[3]Pz@1,3-DCB** is determined as (T$_3$→S$_0$), corresponding to the phosphorescent emission wavelength of 525 nm, which is only 1 nm different from the experimental data. The SOC coefficients of **C[3]Pz** before and after the formation of the complex are compared. It is known that the large $\xi_{ST}$ value is a prerequisite for efficient RTP. As shown in Figure S28 (Supporting Information), the SOC coefficient of **C[3]Pz@1,3-DCB** ($\xi$ (S$_1$, T$_3$), 1.04 cm$^{-1}$) is significantly greater than that of **C[3]Pz** ($\xi$(S$_1$, T$_2$), 0.82 cm$^{-1}$). These results jointly indicate that, thanks to the extensive C−H...$\pi$ interaction and favorable radiation pathways, **C[3]Pz** can achieve more effective ISC and phosphorescent emission in supramolecular system.

## 2.5. Color QR Code and Information Encryption

Finally, on the basis of not changing the excitation wavelength and the host structure, we evaluated the application potential of modulating the host phosphorescent emission by adjusting the structure of the guest molecule. Through solvent evaporation, we conveniently prepared **C[3]Pz@1,2-DCB** and **C[3]Pz@1,3-DCB**, placed them in different models, and obtained corresponding figure as "i ♥ u", where the symbols "i" and "u" are made by **C[3]Pz@1,2-DCB** and **C[3]Pz@1,3-DCB**, respectively, and the symbol "♥" is made by **C[3]Pz** (**Figure 6**a).
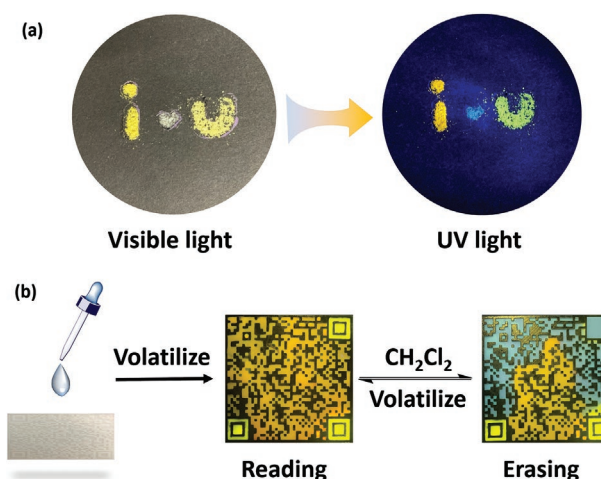


**Figure 6.** a) Photographs of the solid powder of **C[3]Pz**, **C[3]Pz@1,2-DCB**, and **C[3]Pz@1,2-DCB** under visible light and 365 nm UV light. b) Phosphorescence QR code and information storage/encryption of solvent response.

Under the UV lamp, the symbol "♥" emits relatively weak cyan light. Only when **1,2-DCB** and **1,3-DCB** are included in the symbol "♥", the symbol "i" and "u" will emit bright orange light and yellow light, respectively. In addition, we use 3D printing technology to make a 3D model containing QR code on the surface of the plate (Figure 6b). First, **C[3]Pz** was divided into two equal parts and dissolved in dichloromethane solution. Then, **1,2-DCB** and **1,3-DCB** were added to the solution of two parts of **C[3]Pz** respectively, and the mixtures were filled into the 3D model. After the solvent volatilizes, **C[3]Pz@1,2-DCB** and **C[3]Pz@1,3-DCB** attached to the surface of the 3D model will emit yellow and orange light respectively under the irradiation of 365 nm UV light. At this time, a color QR code that can be identified by mobile phone appears. After fumigation with dichloromethane, due to the weakening of the force between the guest molecules and **C[3]Pz** in the solution, the color QR code is destroyed and cannot be recognized by the mobile phone. After the solvent volatilizes, the color QR code can reappear without damage. The above process can be repeated for many times and has good fatigue resistance. The color QR code shows the clear contrast between yellow and orange, which is expected to be further applied to information coding.

## 3. Conclusion

In conclusion, we selectively activated the RTP emission of **C[3]Pz** through the host–guest chemistry strategy. The guest molecule is wrapped in the cavity of **C[3]Pz** as a rivet, which effectively inhibits the rotational vibration of the benzene ring on **C[3]Pz**, thus inhibiting the non-radiative transition, which greatly improves the phosphorescence quantum yield of **C[3]Pz**. **1,2-DCB** and **1,3-DCB** activated RTP emission of **C[3]Pz** at 566 and 524 nm, respectively, with quantum yields of 20.8% and 36.8%. This simple host-guest chemistry strategy breaks the traditional idea of macrocyclic-confined guest phosphorescence emission in supramolecular chemistry, and provides a feasible strategy for guest molecules to induce host phosphorescence emission in the amorphous state.

## 4. Experimental Section

*Preparation of the **C[3]Pz@1,2-DCB** and **C[3]Pz@1,3-DCB***: **C[3]Pz** (10 mg, 0.01 mmol) and **1,2-DCB/1,3-DCB** (1.417 mg, 0.01 mmol) were dissolved in $CH_2Cl_2$(1 mL), **C[3]Pz@1,2-DCB** or **C[3]Pz@1,3-DCB** solid powder was obtained after solvent volatilization. Under the irradiation of 365 nm lamp, **C[3]Pz@1,2-DCB** and **C[3]Pz@1,3-DCB** emitted bright orange and yellow light respectively.

*Theoretical Calculation*: Geometry optimization of **1,2-DCB**, **1,3-DCB**, **C[3]Pz**, **C[3]Pz@1,2-DCB**, and **C[3]Pz@1,3-DCB** were performed in Gaussian 16 program[57] using M06-2X[58] functional with D3 dispersion correction[59] and 6–31+G(d,p) basis set. The TD-DFT and SOC results were given by using M06-2X[58] functional with D3 dispersion correctionand def2-SV(P)[60] basis set (def2/J[61] as auxiliary basis) based on optimized $S_0$ geometry. Single point energy and TD-DFT calculations were carried out using the quantum chemistry program ORCA[62] version 4.2.1. The hole–electron analyses[63] were performed using Multiwfn 3.8 program[64] and the isosurface figure was rendered with VMD.[65]

## Supporting Information

Supporting Information is available from the Wiley Online Library or from the author.

## Acknowledgements

## Conflict of Interest

The authors declare no conflict of interest.

## Data Availability Statement

The data that support the findings of this study are available from the corresponding author upon reasonable request.

## Keywords

[1] Y. Su, S. Z. F. Phua, Y. B. Li, X. J. Zhou, D. Jana, G. F. Liu, W. Q. Lim, W. K. Ong, C. L. Yang, Y. L. Zhao, *Sci. Adv.* **2018**, *4*, eaas9732.

[2] J. M. Song, L. W. Ma, S. Y. Sun, H. Tian, X. Ma, *Angew. Chem., Int. Ed.* **2022**, *61*, e202206157.

[3] D. F. Li, F. F. Lu, J. Wang, W. D. Hu, X. M. Cao, X. Ma, H. Tian, *J. Am. Chem. Soc.* **2018**, *140*, 1916.

[4] M. S. Kwon, Y. Yu, C. Coburn, A. W. Phillips, K. Chung, A. Shanker, J. Jung, G. Kim, K. Pipe, S. R. Forrest, J. H. Youk, J. Gierschner, J. Kim, *Nat. Commun.* **2015**, *6*, 8947.

[5] W. J. Zhao, Z. K. He, B. Z. Tang, *Nat. Rev. Mater.* **2020**, *5*, 869.

[6] W. P. Ye, H. L. Ma, H. F. Shi, H. Wang, A. Q. Lv, L. F. Bian, M. Zhang, C. Q. Ma, K. Ling, M. X. Gu, Y. F. Mao, X. K. Yao, C. F. Gao, K. Shen, W. Y. Jia, J. H. Zhi, S. Z. Cai, Z. C. Song, J. J. Li, Y. Y. Zhang, S. Lu, K. Liu, C. M. Dong, Q. Wang, Y. D. Zhou, W. Yao, Y. J. Zhang, H. M. Zhang, Z. Y. Zhang, X. C. Hang, et al., *Nat. Mater.* **2021**, *20*, 1539.

[7] H. G. Nie, Z. Wei, X. L. Ni, Y. Liu, *Chem. Rev.* **2022**, *122*, 9032.

[8] M. S. Kwon, D. Lee, S. Seo, J. Jung, J. Kim, *Angew. Chem., Int. Ed.* **2014**, *53*, 11177.

[9] X. Ma, C. Xu, J. Wang, H. Tian, *Angew. Chem., Int. Ed.* **2018**, *57*, 10854.

[10] G. Baryshnikov, B. Minaev, H. Agren, *Chem. Rev.* **2017**, *117*, 6500.

[11] Y. Li, M. Gecevicius, J. R. Qiu, *Chem. Soc. Rev.* **2016**, *45*, 2090.

[12] X. W. Liu, W. J. Zhao, Y. Wu, Z. O. Meng, Z. K. He, X. Qi, Y. R. Ren, Z. Q. Yu, B. Z. Tang, *Nat. Commun.* **2022**, *13*, 8.

[13] X. K. Ma, Y. Liu, *Acc. Chem. Res.* **2021**, *54*, 3403.

[14] P. Ceroni, *Chem* **2016**, *1*, 524.

[15] S. Garain, S. Kuila, B. C. Garain, M. Kataria, A. Borah, S. K. Pati, S. J. George, *Angew. Chem.Int. Ed.* **2021**, *60*, 12323.

[16] S. Z. Cai, Z. F. Sun, H. Wang, X. K. Yao, H. L. Ma, W. Y. Jia, S. X. Wang, Z. H. Li, H. F. Shi, Z. F. An, Y. Ishida, T. Aida, W. Huang, *J. Am. Chem. Soc.* **2021**, *143*, 16256.

[17] Z. K. He, W. J. Zhao, J. W. Y. Lam, Q. Peng, H. L. Ma, G. D. Liang, Z. G. Shuai, B. Tang, *Nat. Commun.* **2017**, *8*, 8.

[18] E. Hamzehpoor, C. Ruchlin, Y. Z. Tao, C. H. Liu, H. M. Titi, D. F. Perepichka, *Nat. Chem.* **2022**, *15*, 83.

[19] Y. Y. Gong, L. F. Zhao, Q. Peng, D. Fan, W. Z. Yuan, Y. M. Zhang, B. Z. Tang, *Chem. Sci.* **2015**, *6*, 4438.

[20] Y. Takeda, T. Kaihara, M. Okazaki, H. Higginbotham, P. Data, N. Tohnai, S. Minakata, *Chem. Commun.* **2018**, *54*, 6847.

[21] H. L. Ma, Q. Peng, Z. F. An, W. Huang, Z. G. Shuai, *J. Am. Chem. Soc.* **2019**, *141*, 1010.

[22] Y. T. Wen, H. C. Liu, S. T. Zhang, Y. Gao, Y. Yan, B. Yang, *J. Mater. Chem. C* **2019**, *7*, 12502.

[23] L. T. Xu, G. P. Li, T. Xu, W. D. Zhang, S. K. Zhang, S. W. Yin, Z. F. An, G. He, *Chem. Commun.* **2018**, *54*, 9226.

[24] H. Matsuoka, M. Retegan, L. Schmitt, S. Hoger, F. Neese, O. Schiemann, *J. Am. Chem. Soc.* **2017**, *139*, 12968.

[25] X. P. Zhang, T. Q. Xie, M. X. Cui, L. Yang, X. X. Sun, J. Jiang, G. Q. Zhang, *ACS Appl Mater Interfaces* **2014**, *6*, 2279.

[26] W. H. Huang, B. Chen, G. Q. Zhang, *Chem. - Eur. J.* **2019**, *25*, 12497.

[27] F. Y. Li, S. Guo, Y. Y. Qin, Y. X. Shi, M. P. Han, Z. F. An, S. J. Liu, Q. Zhao, W. Huang, *Adv. Opt. Mater.* **2019**, *7*, 1900511.

[28] E. Lucenti, A. Forni, C. Botta, L. Carlucci, C. Giannini, D. Marinotto, A. Pavanello, A. Previtali, S. Righetto, E. Cariati, *Angew. Chem., Int. Ed.* **2017**, *56*, 16302.

[29] J. Yang, X. Zhen, B. Wang, X. M. Gao, Z. C. Ren, J. Q. Wang, Y. J. Xie, J. R. Li, Q. Peng, K. Y. Pu, Z. Li, *Nat. Commun.* **2018**, *9*, 10.

[30] N. Song, Z. Zhang, P. Liu, Y.-W. Yang, L. Wang, D. Wang, B. Z. Tang, *Adv. Mater.* **2020**, *32*, 2004208.

[31] Z. Y. Yang, Z. Mao, X. P. Zhang, D. P. Ou, Y. X. Mu, Y. Zhang, C. Y. Zhao, S. W. Liu, Z. G. Chi, J. R. Xu, Y. C. Wu, P. Y. Lu, A. Lien, M. R. Bryce, *Angew. Chem., Int. Ed.* **2016**, *55*, 2181.

[32] P. Data, M. Okazaki, S. Minakata, Y. Takeda, *J. Mater. Chem. C* **2019**, *7*, 6616.

[33] Y. Y. Gong, G. Chen, Q. Peng, W. Z. Yuan, Y. J. Xie, S. H. Li, Y. M. Zhang, B. Z. Tang, *Adv. Mater.* **2015**, *27*, 6195.

[34] L. Xiao, Y. S. Wu, J. W. Chen, Z. Y. Yu, Y. P. Liu, J. N. Yao, H. B. Fu, *J. Phys. Chem. A* **2017**, *121*, 8652.

[35] a) O. Bolton, K. Lee, H. J. Kim, K. Y. Lin, J. Kim, *Nat. Chem.* **2011**, *3*, 205; b) B. Zhou, D. P. Yan, *Adv. Funct. Mater.* **2019**, *29*, 1807599.

[36] B. Zhou, D. P. Yan, *Sci China Chem* **2019**, *62*, 291.

[37] Y. Ren, W. B. Dai, S. Guo, L. C. Dong, S. Q. Huang, J. B. Shi, B. Tong, N. R. Hao, L. W. Li, Z. X. Cai, Y. P. Dong, *J. Am. Chem. Soc.* **2022**, *144*, 1361.

[38] Y. Y. Hu, X. Y. Dai, X. Y. Dong, M. Huo, Y. Liu, *Angew. Chem., Int. Ed.* **2022**, *61*, e202213097.

[39] W.-W. Xu, Y. Chen, Y. L. Lu, Y. X. Qin, H. Zhang, X. F. Xu, Y. Liu, *Angew. Chem., Int. Ed.* **2022**, *61*, e202115265.

[40] H. J. Yu, Q. Y. Zhou, X. Y. Dai, F. F. Shen, Y. M. Zhang, X. F. Xu, Y. Liu, *J. Am. Chem. Soc.* **2021**, *143*, 13887.

[41] X. Ma, J. Wang, H. Tian, *Acc. Chem. Res.* **2019**, *52*, 738.

[42] Y. C. Liang, S. S. Gou, K. K. Liu, W. J. Wu, C. Z. Guo, S. Y. Lu, J. H. Zang, X. Y. Wu, Q. Lou, L. Dong, Y. F. Gao, C. X. Shan, *Nano Today* **2020**, *34*, 100900.

[43] Q. Zhou, B. Y. Cao, C. X. Zhu, S. Xu, Y. Y. Gong, W. Z. Yuan, Y. M. Zhang, *Small* **2016**, *12*, 6586.

[44] P. F. Wei, X. P. Zhang, J. K. Liu, G. G. Shan, H. K. Zhang, J. Qi, W. J. Zhao, H. H. Y. Sung, I. D. Williams, J. W. Y. Lam, B. Z. Tang, *Angew. Chem., Int. Ed.* **2020**, *59*, 9293.

[45] W. L. Zhou, Y. Chen, Q. L. Yu, H. Y. Zhang, Z. X. Liu, X. Y. Dai, J. J. Li, Y. Liu, *Nat. Commun.* **2020**, *11*, 4655.

[46] Y. C. Deng, P. Li, J. T. Li, D. L. Sun, H. R. Li, *ACS Appl. Mater. Interfaces* **2021**, *13*, 14420.

[47] S. Garain, B. C. Garain, M. Eswaramoorthy, S. K. Pati, S. J. George, *Angew. Chem., Int. Ed.* **2021**, *60*, 19720.

[48] G. H. Huang, Z. Q. Deng, J. H. Pang, J. H. Li, S. F. Ni, J. A. Li, C. Zhou, H. L. Li, B. J. Xu, L. Dang, M. D. Li, *Adv. Opt. Mater.* **2021**, *9*, 2101337.

[49] Y. H. Sun, Y. Chen, L. N. Jiang, X. Y. Yu, Y. X. Qin, S. P. Wang, Y. Liu, *Adv. Opt. Mater.* **2022**, *10*, 2201330.

[50] X. Yu, W. Liang, Q. Huang, W. Wu, J. J. Chruma, C. Yang, *Chem. Commun.* **2019**, *55*, 3156.

[51] Z. Y. Zhang, Y. Chen, Y. Liu, *Angew. Chem., Int. Ed.* **2019**, *58*, 6028.

[52] H. Y. Zhou, D. W. Zhang, M. Li, C. F. Chen, *Angew. Chem., Int. Ed.* **2022**, *61*, e202117872.

[53] J. Ren, Y. S. Wang, Y. Tian, Z. J. Liu, X. H. Xiao, J. Yang, M. M. Fang, Z. Li, *Angew. Chem., Int. Ed.* **2021**, *60*, 12335.

[54] Y. S. Wang, J. Yang, M. M. Fang, Y. X. Gong, J. Ren, L. J. Tu, B. Z. Tang, Z. Li, *Adv. Funct. Mater.* **2021**, *31*, 2101719.

[55] Z. L. Xie, X. Y. Zhang, H. L. Wang, C. Huang, H. D. Sun, M. Y. Dong, L. Ji, Z. F. An, T. Yu, W. Huang, *Nat. Commun.* **2021**, *12*, 3522.

[56] H. T. Z. Zhu, I. Badia-Dominguez, B. B. Shi, Q. Li, P. F. Wei, H. Xing, M. C. R. Delgado, F. H. Huang, *J. Am. Chem. Soc.* **2021**, *143*, 2164.

[57] M. J. Frisch, G. W. Trucks, H. B. Schlegel, G. E. Scuseria, M. A. Robb, J. R. Cheeseman, G. Scalmani, V. Barone, G. A. Petersson, H. Nakatsuji, X. Li, M. Caricato, A. V. Marenich, J. Bloino, B. G. Janesko, R. Gomperts, B. Mennucci, H. P. Hratchian, J. V. Ortiz, A. F. Izmaylov, J. L. Sonnenberg, D. W. Young, F. Ding, F. Lipparini, F. Egidi, J. Goings, B. Peng, A. Petrone, T. Henderson, D. Ranasinghe, et al., *Gaussian 16*, Revision A.03, Gaussian, Inc., Wallingford, CT **2016**.

[58] Y. Zhao, D. G. Truhlar, *Theor Chem Acc* **2008**, *120*, 215.

[59] S. Grimme, J. Antony, S. Ehrlich, H. J. Krieg, *Chem. Phys.* **2010**, *132*, 154104.

[60] F. Weigend, R. Ahlrichs, *Phys Chem Chem Phys* **2005**, *7*, 3297.

[61] F. Weigend, *Phys Chem Chem Phys* **2006**, *8*, 1057.

[62] F. Neese, W. Interdiscip, *Wiley Interdiscip. Rev.: Comput. Mol. Sci.* **2012**, *2*, 73.

[63] Z. Liu, T. Lu, Q. Chen, *Carbon.* **2020**, *165*, 461.

[64] T. Lu, F. Chen, *J. Comput. Chem.* **2012**, *33*, 580.

[65] W. Humphrey, A. Dalke, K. Schulten, *J. Molec. Graphics.* **1996**, *14*, 33.